Caving 2022 - Y Potvin (ed.)

doi:10.36487/ACG_repo/2205_12

Shear performance of yielding self-drilling anchors under controlled conditions

G Knox *University of Toronto, Canada*

J Hadjigeorgiou *University of Toronto, Canada*

Abstract

The traditional installation of grouted rockbolts requires a support hole to be pre-drilled followed by the installation of a cementitious or resin grout. The rockbolt is then inserted into the grout. In highly stressed or poor ground, the presence of fractures, shear features and altered rock can lead to unravelling of the support hole and result in blockages and grout losses. Consequently, the support holes are often redrilled, resulting in oversized holes, increased installation times, and poor installation quality.

Replacing the conventional drill string with a self-drilling anchor (SDA) improves both the quality and advancement rate of installation. These are critical considerations in poor ground. The SDA rockbolt is coupled to the rock drill, drilled to depth, then decoupled and post grouted. This one-step installation method overcomes the challenges of drilling into fractured rock where hole closures and grout losses are common. The operational advantages of the application of a one-step system using self-drilling anchors have recently been demonstrated in two caving operations, Oyu Tolgoi mine in Mongolia and Malmberget mine in Sweden.

A yielding SDA offers additional performance benefits when in squeezing rock or seismic prone ground. There is limited data on the response of yielding self-drilling anchors to tensile and shear loading under controlled laboratory conditions. The undertaken experimental program has investigated the behaviour of a yielding SDA under tensile and shear loads. This contributes to an improved understanding of the response of self-drilling anchors under a single loading mechanism and can provide an indication of performance in highly stressed and fractured rock observed in caving operations and deep underground mines.

Keywords: *self-drilling anchors, shear testing, bulk resin systems, mechanised mining*

1 Introduction

To optimise the performance of a ground support system, it is important to match the response of the ground support to the anticipated rock mass failure mechanism. There are several conventional and yielding or energy absorbing rockbolts that can be used as part of a support strategy for a range of ground conditions and rock mass failure mechanisms. In ground conditions where large deformations are anticipated, such as squeezing or seismic conditions, the application of yielding rockbolts is considered best practice (Potvin & Hadjigeorgiou 2020).

A practical consideration, irrespective of the type of rockbolt used, is the ability to install the reinforcement elements in pre-drilled holes in the rock mass. Drilling the holes in heavily fractured or poor ground can be a challenge. For example, Bray et al. (2019) report on the challenges noted when installing conventional grouted bolts in the biotite schists at LKAB's Malmberget mine in Sweden. Watt et al. (2018) also reported on problems encountered in the installation of resin cartridge rockbolts at Rio Tinto's Oyu Tolgoi mine in Mongolia. At both sites, problems encountered included hole closures that prevented the installation of the rockbolts and/or voids and blown out holes resulting as shown in Figure 1. The effect of the variations in the support hole result in ineffective installation reducing the anchor strength capacity of the rockbolts. In this context, the use of self-drilling anchors (SDA) is an attractive option that can overcome issues with installation holes in poor quality ground.

Figure 1 Examples of hole closure and collapse in fractured ground conditions (Watt et al. 2018)

Following SDA trials at Oyu Tolgoi, Watt et al. (2018) reported an improvement in installation quality, while Bray et al. (2019) observed greater installation efficiency using SDAs at Malmberget. Furthermore, since SDAs remain in the hole during installation, they have the additional advantage of mitigating issues with blockages of the bore hole.

This paper recognises the potential of operational benefits of SDAs in poor quality ground conditions. The focus of this investigation, however, is in quantifying the capacity of a yielding SDA under pure shear and tensile conditions. This is an area where there is a currently scarcity of data to support the design process. Of further interest is exploring the relationship between ultimate tensile and shear strength.

2 Self-drilling anchors

Both cement and resin grouted SDAs have been employed in tunnelling for a long time. Resin grouted SDAs are increasingly popular in mining as they have been shown adaptable for fractured and friable ground conditions where hole closures, voids and fractures are common. This is of particular importance in caving operations.

Historically, SDA installation has been a two-step process: self-drilling, followed up with the injection of cementitious grout or resin. The development of 'one-step' bolting systems, e.g. the Epiroc Boltec, have provided further opportunities for the more widespread application of SDA as they provide greater installation efficiency.

The installation process for SDA is illustrated in Figure 2, noting that the rockbolt is coupled to the rock drill. The drilling process uses a combination of percussion and rotation applied to the proximal end of the rockbolt. This results in the fracturing of the rock and flushing of waste material out of the support hole by flushing water down the core of the rockbolt. When the washer plate is in firm contact with the rock mass, the rockbolt is deemed to be drilled to the correct depth and the rock drill is decoupled. Resin is then injected through the core of the rockbolt, to the distal end of the support hole, filling the annulus between the rockbolt and the support hole. The resin injection is halted when resin is observed at the periphery of the washer plate. The post injection of resin ensures variations in hole size and voids surrounding the rockbolt are accommodated for, and a full column bond is achieved. The rockbolt is held in place by the bolter during the curing period of the resin, completing the installation. The development of one-step bolting systems allows for this process to be conducted without repositioning the boom on the bolter.

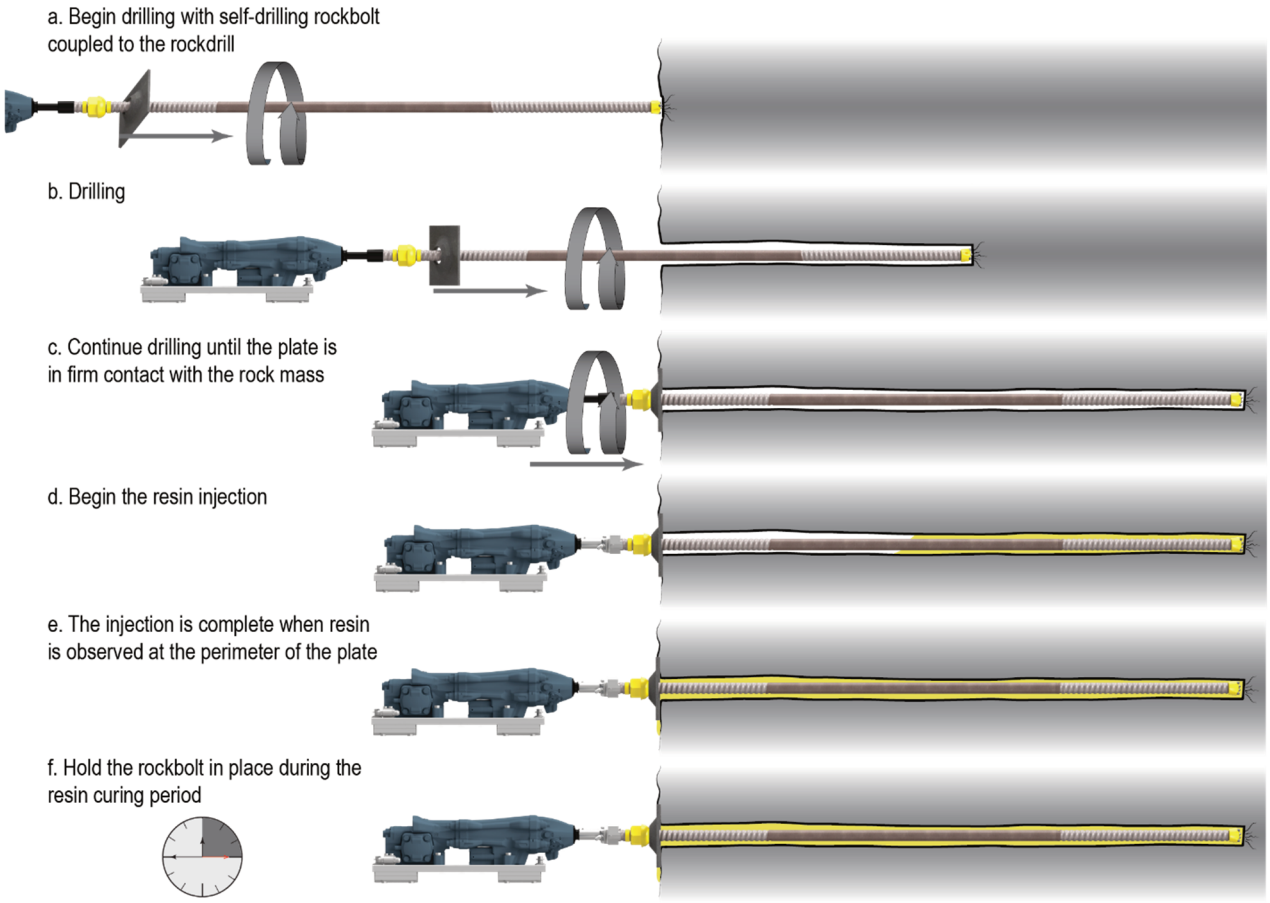

Figure 2 One-step installation process for an SDA

2.1 Yielding SDA

Yielding SDAs are a sub-group of SDAs employed where it is necessary to overcome installation issues in fractured and friable ground, and have the energy-absorbing capacity to perform adequately under seismic loads and squeezing ground conditions. An example of a yielding resin grouted SDA is the R28 BoraBolt designed and manufactured by Epiroc (2022b) consisting of two 600 mm long threaded sections rolled onto a Ø28 mm tube, is shown in Figure 3. A smooth section of steel is modified to produce one or more anchor points along the length of the rockbolt. The rockbolt is installed with cementitious or resin-based grout which is mechanically coupled to the perimeter of the support hole and the anchor points on the rockbolt.

Figure 3 An example of an SDA: the R28 BoraBolt

In the R28 BoraBolt, the yielding mechanism is achieved when the smooth, highly deformable section between the threaded sections decouples from the grouting medium (resin) and elongates when load is applied to the rockbolt. In effect, the threaded sections at the two ends of the bar have a similar role as the anchors in paddled energy absorbing rockbolts (Figure 4). In both cases, energy is dissipated by the deformation of the smooth section between the anchor points.

The rock–grout and grout–rockbolt interfaces form the load transfer mechanism, preventing the dilation of joint intersected by the rockbolt. The length of steel between the anchor points on the rockbolt decouples from the grout medium, increasing the length of steel mobilised. Consequently, the strain is uniformly distributed along the smooth length of steel between the anchor points as illustrated in Figure 4 and the deformation capacity of the rockbolt governed by the mechanical properties of the steel under pure tensile loading.

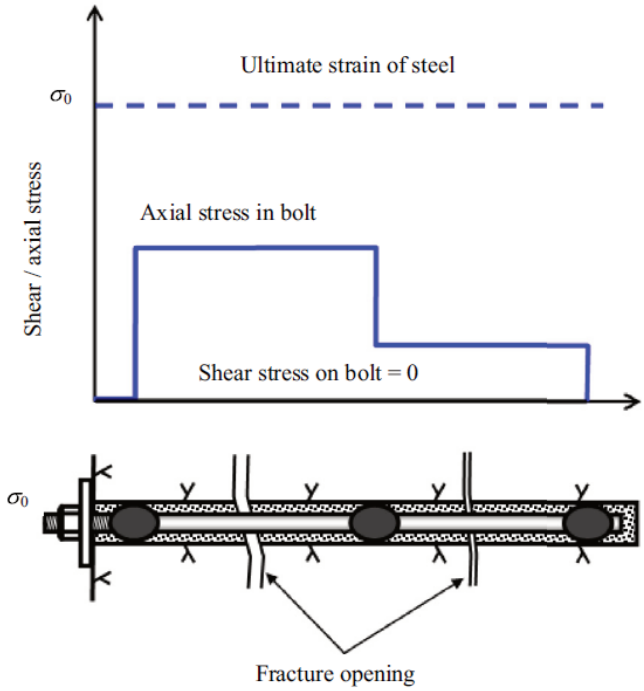

Figure 4 Theoretical stress distribution of a multi-point anchored rockbolt (Li et al. 2014)

3 Rockbolt response to tensile and shear load

Li (2010) provided a series of field observations on the loading conditions and failure modes of rockbolts in high stress conditions in cut and fill mines, concluding that they are subjected to both pull and shear loads. Thompson et al. (2012), suggested that the loading mechanisms can be more complex and difficult to interpret. An understanding of the performance of a rockbolt can arguably be obtained by a series of tests in a controlled environment whereby a single loading mechanism is isolated and investigated.

A review of laboratory results on the pull capacity of both conventional and energy absorbing rockbolts has been provided by Li et al. (2014). Hadjigeorgiou & Tomasone (2018) have presented the results of in situ pull tests in Canadian mines.

A review of laboratory test results of grouted rockbolts suggested that a rockbolt does not fail under pure shear, rather the fracturing of the grout and rock mass surrounding the collar of the support hole results in a bending moment being placed on the rockbolt. Consequently, the mechanical properties of the rockbolt steel are not the only factor that defines the shear capacity of a rockbolt.

Hartman & Hebblewhite (2003) provided a review of earlier shear tests on rockbolts suggesting that several parameters such as rock mass strength, reinforcement design and loading conditions could potentially influence the performance of rock reinforcement elements in a jointed rock mass subjected to shear loading. There is relatively little information on the shear capacity of rockbolts, although Stjern (1995), Li et al. (2014), Chen & Li (2014, 2015), and Hagen et al. (2019) have provided valuable insights.

To investigate the shear performance of rockbolts, Stjern (1995) developed a testing rig to conduct index shear tests under a controlled environment. This is referred to as the SINTEF Rockbolt Pull Tester and was also used by Chen & Li (2015) to investigate the performance in shear of yielding rockbolts. In this setup, a

rockbolt is installed into a borehole drilled into a pair of concrete blocks; the blocks are driven individually loading the sample in either shear or tension.

Of interest is the observation by Stjern (1995) that for conventional rockbolts the ultimate shear resistance of a rockbolt is between 80 and 100% of the ultimate tensile capacity depending on the strength of the host rock material. Chen & Li (2014, 2015) observed a difference in behaviour between conventional (rebar) and paddled rockbolts when comparing response to shear and tensile loading (displacement at ultimate load and ultimate load). The displacement at ultimate shear load decreased in comparison to the displacement at ultimate tensile load when considering a yielding paddled rockbolt such as the D-Bolt and increased when considering a conventional rebar rockbolt.

None of the reported shear tests involved SDA. In fact, there is very little information on the shear capacity of SDAs or their relative value to their tensile capacity. Watt et al. (2018) presented an estimated shear performance of the anchor as 70% of the ultimate tensile strength (0.7 × UTS), but there is no explanation on how this estimate was made.

4 Experimental program

The experimental program aimed at quantifying the tensile and shear capacity of a yielding SDA and explore the relationship between tensile and shear load capacity. To these purposes a comprehensive experimental investigation was designed aiming at reducing uncertainty by controlling the sample preparation and sourcing of the rockbolts used.

4.1 Yielding SDA and resin

This experimental program used 2.4 m long R28 BoraBolt yielding SDAs as shown in Figure 3 and the Potentia Thixo F60 resin. When installed as a one-step SDA, a Ø35 mm drill bit is fixed to the distal end of the rockbolt. This investigation used the two-step variant of the rockbolt: the drill bit was emitted from the rockbolt assembly. The Potentia Thixo resin is a two-component bulk resin, supplied as a resin and a catalyst. The two components are mixed in a 1:1 ratio prior to injection into the rockbolt. The tack-free time (TFT) of the resin is 60 seconds at a resin temperature of 20°C, the TFT is inversely proportional to the resin temperature.

4.2 Testing apparatus

All tests were conducted using the Epiroc Combination Shear and Tensile (CST) Rockbolt Pull Tester, seen in Figure 5. The rig was constructed using the same principles of the SINTEF rig (Stjern 1995), with modifications to the hydraulic control system, sample length, and shear capacity.

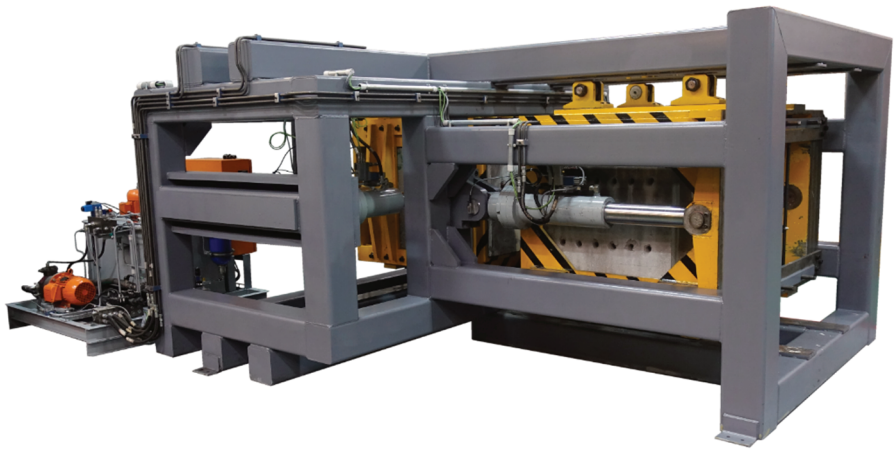

Figure 5 Epiroc Combination Shear and Tensile Rockbolt Pull Tester (Epiroc 2022a)

The Epiroc CST Rockbolt Pull Tester consists of a loading frame, a shear and tensile trolley, concrete blocks, and a hydraulic power pack. Each of the trolleys are driven by two independently controlled hydraulic

cylinders. Load cells are installed between the cylinders and the load frame and linear variable differential transformers (LVDTs) within the cylinders as illustrated in Figure 6. The instrumentation configuration and controller enable both loading and displacement rate control. External LVDTs are strategically located to record the movement of the concrete blocks relative to the trolley and the displacement of the shear trolley relative to the loading frame in the tensile direction. The capacity specifications of the equipment are summarised in Table 1.

Table 1 Epiroc Rockbolt Pull Tester

Parameter	Capacity
Shear load (kN)	500
Shear displacement (mm)	300
Tensile load (kN)	500
Tensile displacement (mm)	500
Max. bolt length (mm)	2,400
Bond length (mm)	1,200

As illustrated in Figure 6, the rockbolt is installed through the two concrete blocks (tensile and shear blocks). During the loading sequence, the load trolleys are driven apart by the hydraulic cylinders. The translation is determined by the loading profile configured, resulting in a combination loading which could range from pure tensile (0°) to pure shear loading (90°). During loading, the data are recorded at 100 Hz and processed to determine the load response of the rockbolt.

A shear test under controlled conditions in a laboratory is an index test. Factors such as joint roughness, infilling, lithology, and normal pressure contribute to variations in the shear resistance of a joint. The aim of the test is to evaluate the rockbolt. Consequently, prior to applying a shear load, a displacement of 3 mm is applied to the tensile block. This ensures that there is a separation between the two blocks, hence the friction between the blocks is discounted from the result.

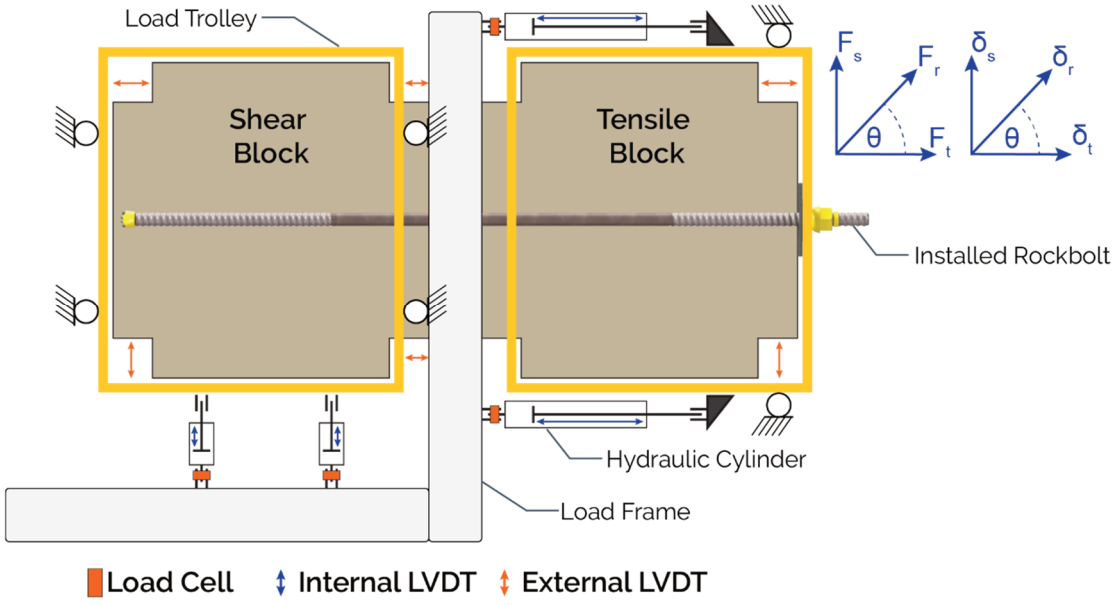

Figure 6 Schematic of the Epiroc RGU Combination Shear Tensile Rockbolt Pull Tester

4.3 Sample preparation

The host material and grouting medium influence the shear performance of a rockbolt. Consequently, in this investigation significant emphasis was placed on the preparation of the concrete blocks, installation of the rockbolt, and quality of the grouting medium. This has ensured that the properties of each component of the system could be quantified.

The concrete blocks are cast using a mould designed for the profile of the trolleys. Once the premixed concrete has been poured and vibrated to remove air from the mixture the block was left to cure for a period of 28 days. A jig is placed over one of the concrete blocks to ensure equal 150 mm spacing between the support holes both horizontally and vertically. A S25 pneumatic rock drill is used to drill the holes with a Ø36 mm diameter, seven button knock-off bit. As the drill bit exits the concrete block, a significant breakout of the concrete surrounding the collar of the hole occurs, as illustrated in Figure 7a. To ensure that the break does not affect the shear performance of the rockbolt, the first block is rotated (Figure 7b) to ensure that the borehole diameter is controlled at the shear interface. The drill steel is then inserted through the first block during the drilling of the second block to ensure the alignment of the holes between the two blocks is maintained (Figure 7c). A total of 21 holes are drilled. The holes on the perimeter of the concrete blocks are reserved for tensile tests and the central holes used for shear tests. This prevents failure of the concrete blocks at the joint.

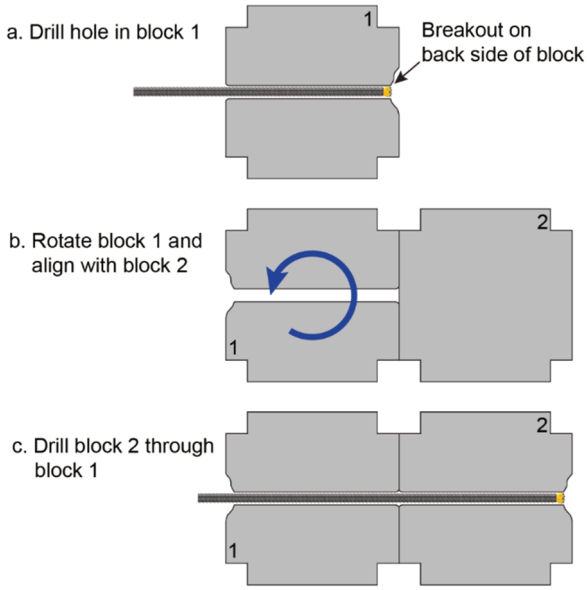

Figure 7 Top view illustration of the process for drilling holes in the concrete blocks for rockbolt pull testing

The 3,200 kg concrete blocks are then installed into the trolleys, seated, and fixed into place. Prior to installing the rockbolt through the specified support hole, the distal portion of the hole is plugged, and a gasket installed at the joint between the two concrete blocks. The gasket prevents the pressurised resin from penetrating the joint. The trolleys are then positioned using the hydraulic cylinders ensuring a compressive force is applied at the joint. The rockbolt, without the drill bit installed, is then inserted into the predrilled hole and injected with resin.

Polyurea silicate resin requires a 1:1 volumetric ratio between the resin and catalyst. Deviations from the ratio results in a reduction in cured resin strength. Epiroc developed a resin mixing and injection system for the Boltec. The closed loop system controls the flow rate of each component separately ensuring the ratio is maintained. A simplified schematic of the system is illustrated in Figure 8. A replica of the system has been built in the Epiroc Application Centre and used to pump the Potentia Thixo F60 resin for this investigation. At the start, up to five 40 mm cubes of resin were poured for compressive strength verification testing.

A curing time of one hour was used prior to testing each sample. Table 2 defines the pump parameters used during the resin injection.

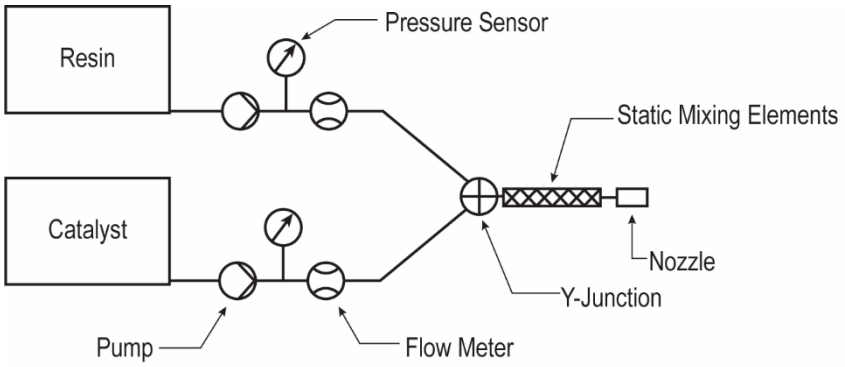

Figure 8 Simplified schematic of the resin pumping system

Table 2 Potentia Thixo Resin properties used in the tests

Parameter	Value
Mixing ratio (A/B)	1:1
Flow rate	8.5 L/min
Number of mixer elements	14
Temperature	23°C

5 Results of the experimental program

5.1 Material control

In a laboratory test, there are several variables that can influence the shear performance of a rockbolt including the properties of host material, anchoring medium, and steel from which the rockbolt is produced (Hartmann & Hebblewhite 2003). During this investigation, the properties of each component of the setup were confirmed. The unconfined compressive strength (UCS) of the concrete (host material) and the resin (anchoring medium) were determined using 100 mm and 40 mm cubes respectively. Two samples of the grout were tested, and five samples of the resin were cast. The average results for the UCS tests are presented in Table 3, and the stress–strain curve for the resin is presented in Figure 9a.

Table 3 Summary of unconfined compressive strength results

Material	Number of samples	Avg. UCS (MPa)
AfriSam Ready Mix	2	90
Potentia Thixo F60	5	37

All six samples of the BoraBolt rockbolts were manufactured from the same batch of steel. As part of the quality assurance for this experimental investigation, the mechanical properties of the steel were verified. The ultimate tensile load and elongation at rupture were determined in accordance with the International Organization for Standardization (2019) method for tensile testing. Based on an average of five samples the ultimate tensile load was determined to be 242 kN with a strain of 25% at rupture. The uniform response of the rockbolts is shown in the load–displacement curve plotted in Figure 9b.

In addition to the verification of the mechanical properties, the diameter of the support holes was measured. The diameter of the support holes at the joint interface was found to be in the range of Ø35 to Ø38 mm with an average of Ø36 mm.

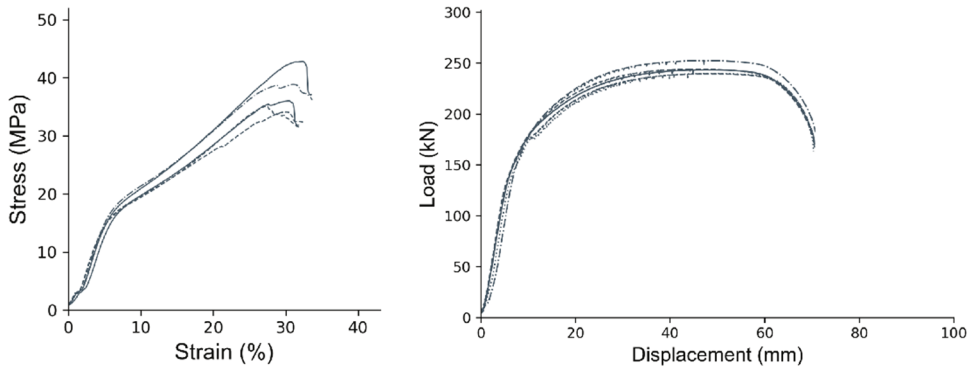

Figure 9 Response curves for (a) the compressive loading of the Potentia Thixo Resin and (b) tensile loading of the steel tube used to produce the BoraBolt

5.2 Rockbolt pull test results

The results of the testing program are presented in Table 4. The first batch of BoraBolts (BB2824-S01 – S03) were subjected to a pure shear loading (90°), and a second set of rockbolts (BB2824-T01 – T03) were loaded using a pure tensile loading sequence (0°). The results of both the shear and tensile results are represented by the ultimate load ($F_{x\,\max}$) and the displacement at ultimate load ($\delta_{x\,F_{x\,\max}}$). The support resistance capacity of the rockbolt diminished between the $\delta_{x\,F_{x\,\max}}$ and the displacement at rupture ($\delta_{x\,max}$), consequently this represents the ultimate working capacity of the rockbolt.

Table 4 Summary of individual BoraBolt R28 by 2.4 m pull test results

Sample reference	Mechanism	Loading angle	$\delta_{t\,F_t max}$ (mm)	$F_{t\,max}$ (kN)	$\delta_{s\,F_s max}$ (mm)	$F_{s\,max}$ (kN)
BB2824-S01	Pure shear	90°	-3	38.2	45	202
BB2824-S02	Pure shear	90°	0	13.8	49	221
BB2824-S03	Pure shear	90°	-2	25.9	62	222
BB2824-T01	Pure tension	0°	180	231	-0	5
BB2824-T02	Pure tension	0°	168	234	-0	2
BB2824-T03	Pure tension	0°	200	235	1	6

The displacement of the trolleys is controlled by the hydraulic cylinders internal LVDTs. The movement of the concrete blocks relative to the trolleys and the loading frame (Figure 6) is recorded using the external LVDTs and correct for in the presented results. Therefore, zero movement of the trolley with a negative displacement of the blocks results in a negative final displacement on an axis. This was observed in samples BB2824 S01 and S03, with a negative tensile displacement (perpendicular to direction of loading).

A comparative load–displacement response comparing the shear and tensile response is plotted in Figure 10. The results are consistent with tests on other rockbolts (e.g. Stjern (1995) where the ultimate shear load is attained at relatively lower values than at rupture under tensile load).

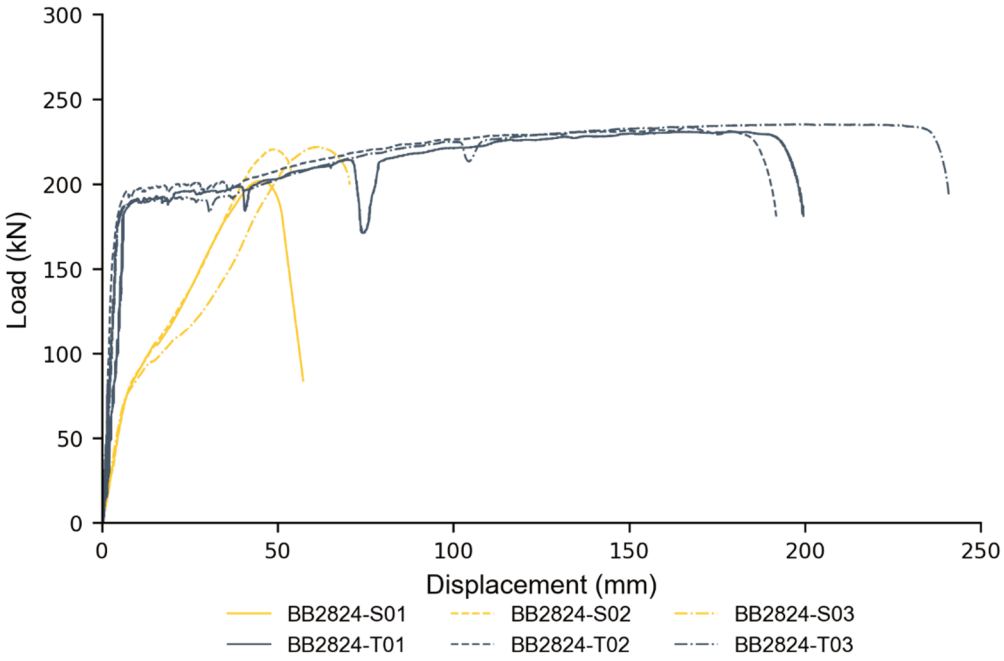

Figure 10 Load–displacement response of the R28 by 2.4 m BoraBolt

A summary of the results is given in Table 5. The shear displacement $\delta_{s\ F_s max}$ was determined to be 29% of the tensile displacement at ultimate tensile load ($\delta_{t\ F_t max}$). Similarly, a reduction in the ultimate shear load ($F_{s\ max}$), 92% of the ultimate tensile load ($F_{t\ max}$), was observed. The ratio between the ultimate shear load and ultimate tensile load is considerably higher than the estimate of 70% provided by Watt et al. (2018).

Table 5 Summary of individual BoraBolt R28 by 2.4 m Pull Test Results

Rockbolt	Avg. $F_{s\ max}$ (kN)	Avg.$\delta_{s\ F_s max}$ (mm)	Avg. $F_{t\ max}$ (kN)	Avg. $\delta_{t\ F_t max}$ (mm)	F_s/F_t	δ_s/δ_t
BoraBolt R28 by 2.4 m	215	52	233	182	0.92	0.29

A macroscopic investigation was undertaken of the fracture surface of the rockbolts following the tensile and shear tests. Figure 11 illustrates the rockbolt deformation profile and movement of the rockbolt within the support hole for the matching surfaces of the SDA. For reference purposes, Figure 11 shows the segment of the bolt installed in the shear block (Figure 6) and Figure 11b in the tensile (stationary) block of the testing setup. It was clearly observed that the rockbolt repositioned and deformed from the original position and profile demarcated by the red dashed circle to the perimeter of the original borehole profile (delineated by the green dashed circle).

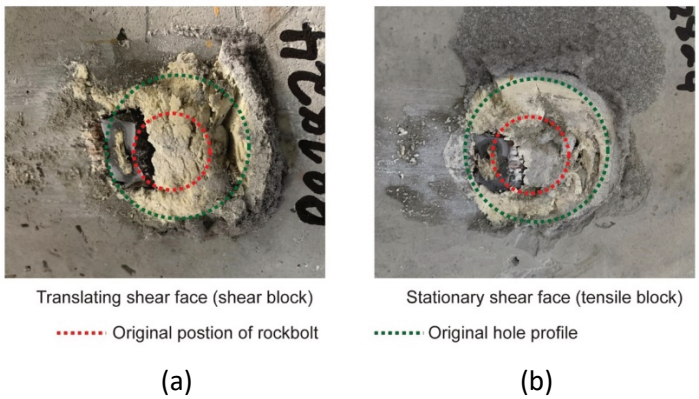

Figure 11 Fracture surface of a sheared SDA; (a) Shear block; (b) Tensile block

Figure 12 presents the fracture surface of the SDA following the pull test. This is a typical ductile necking and eventual rupture resulting in a cup and cone illustrated in Figure 12, when a tensile load was applied.

Figure 12 Fracture surface of an SDA following a tensile test

6 Discussion

Following the tests to demonstrate the consistency of the mechanical properties of the resin and steel used to manufacture the BoraBolt it was anticipated that the resin strength would be consistent along the length of the rockbolt.

Reviewing the load–displacement response of the tested SDA, a variation in the ultimate shear load was noted with S01 recording an ultimate shear load of 202 kN as opposed to the 220.6 and 220.0 kN recorded for samples S02 and S03 respectively. Figure 10 illustrates an inflection point at 80 kN in the shear response followed by a softening of the stiffness. All three samples demonstrated a similar response at the 80 kN inflection point. However, the response of samples S01 and S02 was stiffer than S03 between the inflection point and the ultimate shear load. This may have contributed to the additional 13 mm of displacement recorded between samples S02 and S03.

As anticipated, the position of the axis of the rockbolt shifted within the support hole, with the rockbolt being located against the perimeter of the support hole. In addition, the circular profile deformed during the shear loading, transforming the circular profile of the tube into an elliptical profile. This transformation is illustrated in Figure 11.

A reduction in the shear displacement was noted when compared to the tensile displacement for a yielding rockbolt. This is consistent with the work by Chen & Li (2014). As a result of the consistency of the mechanical properties of the steel, it can be interpreted that the reduction in displacement can be attributed to a reduction in the length of steel mobilised during shear loading. The bending generated during shear loading isolates the length of the smooth section mobilised during the loading, resulting in the reduction.

During the shear loading of a rockbolt a component of the load response is in tension. The magnitude of the tensile load varied between the shear samples (BB2824-S01 – S03). The maximum recorded tensile load was noted on S01, which recorded the lowest shear load of the three samples. Subsequently, S01 recorded the lowest resultant load.

7 Conclusion

This paper presented the results of an experimental investigation on the shear strength of SDA in a controlled laboratory investigation. Of interest to the investigation was a determination of the relationship between the ultimate shear load and ultimate tensile load. To these purposes, considerable effort was directed

towards the material sourcing and experimental procedure to ensure that all variations were attributed to the loading mechanism.

The ultimate tensile strength of the R28 BoraBolt was 233 kN with a displacement at maximum tensile load of 182 mm. The ultimate shear resistance of the R28 was 215 kN (0.92 × UTL), with a shear displacement at maximum shear load of 52 mm (0.28 x $\delta_{t\ F_t\ max}$). The noted reduction in displacement is an indication that the shear loading of a rockbolt reduces the loaded length of steel; consequently this may affect the ultimate tensile displacement in a multi-modal loading case. The ultimate shear load of the tested yielding SDA was 92% of the ultimate tensile load. This is higher than the 70% previously assumed for SDAs and may have significant implications.

Acknowledgement

The authors acknowledge Epiroc Ground Support for providing access to the testing facility, the rockbolts and resin used in this testing campaign. The contribution of Shane Koapeng and his team in operating the testing facility is gratefully acknowledged.

References

Bray, P, Johnsson, A, & Shcunnesson, H 2019 'Rock reinforcement solutions case study: Malmberget iron ore mine, Sweden', in W Joughin (ed), *Proceedings of the Ninth International Conference on Deep and High Stress Mining*, The Southern African Institute of Mining and Metallurgy, Johannesburg, pp. 191–204.

Chen, Y & Li, C 2014 'Performance of fully encapsulated rebar bolts and D-Bolts under combined pull-and-shear loading', *Tunnelling and Underground Space Technology*, vol. 45, pp. 99–106.

Chen, Y & Li, C 2015 'Influences of loading conditions and rock strength to the performance of rock bolts', *Geotechnical Testing Journal*, vol. 38 no. 2, pp. 208–218.

Epiroc 2022a, Epiroc, Stockholm, viewed 10 June 2022, https://www.epiroc.com/en-za/products/rock-drilling-tools/ground-support/research-and-development-centre

Epiroc 2022b, Epiroc, Stockholm, viewed 20 May 2022, https://www.epiroc.com/en-za/products/rock-drilling-tools/ground-support/energy-absorbing-rockbolts/borabolt

Hadjigeorgiou, J & Tomasone, P 2018, 'Characterising the behaviour of rockbolts based on in situ pull tests', in Y Potvin & J Jakubec (eds), *Caving 2018: Proceedings of the Fourth International Symposium on Block and Sublevel Caving*, Australian Centre for Geomechanics, Perth, pp. 727–734.

Hagen, S, Larsen, T, Berghorst, A, & Knox, G 2019, 'Laboratory full-scale rock bolt testing: analysis of recent results', in W Joughin (ed), *Proceedings of the Ninth International Conference on Deep and High Stress Mining*, The Southern African Institute of Mining and Metallurgy, Johannesburg, pp. 217–230.

Hartmann, W & Hebblewhite, B 2003 'Understanding the performance of rock reinforcement elements under shear loading through laboratory testing - A 30 year history', *Proceedings 1st AGCM Conference,* Sydney.

International Organization for Standardization 2019, *Metallic materials - Tensile Testing – Part 1: Method of test at room temperature (ISO 6892-1:2019)*, International Organization for Standardization, Geneva.

Li, C 2010, 'A new energy-absorbing bolt for rock support in high stress rock masses', *International Jounrnal of Rock Machanics & Mining Sciences*, vol. 47, pp. 396–404.

Li, C, Stjern, G & Myrvang, A 2014, 'A review on the performance of conventional and energy-absorbing rockbolts', *Journal of Rock Mechanics and Geotechnical Engineering*, pp. 315–327.

Potvin, Y & Hadjigeorgiou, J 2020, *Ground Support for underground mines*, Australian Centre for Geomechanics, Perth.

Stjern, G 1995, *Practical Performance of Rockbolts*, PhD thesis, University of Science and Technology, Tronheim.

Thompson, A, Villaescusa, E & Windsor, C 2012, 'Ground support terminology and classification: an update', *Geotechnical and Geological Engineering*, vol. 30 no. 3, pp. 553–580.

Watt, G, Roberts, T & Faulkner, D 2018, 'Single pass drill, install and inject self-drilling resin bolt applications in poor ground', *Proceedings of The Fourth Australasian Ground Control in Mining Conference Proceedings*, The Australasian Institute of Mining and Metallurgy, Melbourne, pp. 323–343.